Article:
Konki, J., Sulignano, B., Greenlees, P. T. et al. (27 more authors) (2018) In-beam spectroscopic study of 244Cf. Physical Review C - Nuclear Physics. 024306. ISSN 1089-490X

https://doi.org/10.1103/PhysRevC.97.024306

In-beam spectroscopic study of ^{244}Cf

J. Konki,[1,*] B. Sulignano,[2] P. T. Greenlees,[1] Ch. Theisen,[2] K. Auranen,[1,†] H. Badran,[1] R. Briselet,[2] D. M. Cox,[1] F. Defranchi Bisso,[1] J. Dobaczewski,[1,3,4,5] T. Grahn,[1] A. Herzán,[1,‡] R.-D. Herzberg,[6] R. Julin,[1] S. Juutinen,[1] J. Khuyagbaatar,[7,8] M. Leino,[1] A. Lightfoot,[1] J. Pakarinen,[1] P. Papadakis,[1] J. Partanen,[1] P. Rahkila,[1] M. Sandzelius,[1] J. Sarén,[1] C. Scholey,[1] Y. Shi,[9,1] M. Smolen,[10] J. Sorri,[1] S. Stolze,[1] and J. Uusitalo[1]

[1] *University of Jyvaskyla, Department of Physics, P.O. Box 35, FI-40014 Jyvaskyla, Finland*
[2] *IRFU, CEA, Université Paris-Saclay, 91191 Gif-sur-Yvette, France*
[3] *Helsinki Institute of Physics, P.O. Box 64, FI-00014 University of Helsinki, Finland*
[4] *University of York, Department of Physics, Heslington, York YO10 5DD, UK*
[5] *University of Warsaw, Institute of Theoretical Physics, Faculty of Physics, ul. Pasteura 5, PL-02-093 Warsaw, Poland*
[6] *University of Liverpool, Department of Physics, Oliver Lodge Laboratory, Liverpool L69 7ZE, UK*
[7] *Helmholtz Institute Mainz, 55099 Mainz, Germany*
[8] *GSI Helmholtzzentrum für Schwerionenforschung GmbH, 64291 Darmstadt, Germany*
[9] *Department of Physics, Harbin Institute of Technology, Harbin 150001, People's Republic of China*
[10] *University of the West of Scotland, School of Engineering and Computing, Paisley PA1 2BE, UK*

(Dated: January 10, 2018)

The ground-state rotational band of the neutron-deficient californium ($Z = 98$) isotope ^{244}Cf was identified for the first time and measured up to a tentative spin and parity of $I^\pi = 20^+$. The observation of the rotational band indicates that the nucleus is deformed. The kinematic and dynamic moments of inertia were deduced from the measured γ-ray transition energies. The behaviour of the dynamic moment of inertia revealed an up-bend due to a possible alignment of coupled nucleons in high-j orbitals starting at a rotational frequency of about $\hbar\omega = 0.20$ MeV. The results were compared to the systematic behaviour of the even-even $N = 146$ isotones as well as to available theoretical calculations that have been performed for nuclei in the region.

PACS numbers: 27.90.+b, 21.10.-k, 23.20.Lv

I. INTRODUCTION

The stability of the heaviest elements with $Z > 100$ against fission is only due to nuclear shell effects. The possible existence of a non-zero fission barrier in these nuclei can be understood in terms of a shell correction applied in addition to the energy from the liquid-drop model resulting in lifetimes long enough to be experimentally observed. For decades, defining the limits of the stability of the atomic nucleus has been of great interest reflected by the persistent studies of the transfermium superheavy nuclei (SHN). In order to be able to constrain the various theoretical models that predict different locations for the next spherical shell closure beyond $Z = 82$ and $N = 126$, *i.e.*, the so-called island of stability, more information on the ordering and spacing of the single-particle orbitals and structure is needed.

Decay and in-beam spectroscopy have been applied extensively in the recent years to study the structure of deformed heavy nuclei [1]. With in-beam γ-ray spectroscopy it is possible to probe the spin dependent properties of the deformed nuclei for instance when they rotate or vibrate. The rotational bands and their moments of inertia provide information on deformation, particles that are active in the orbitals around the Fermi surface and deformed shell closures. The variation of the moment of inertia as a function of spin is sensitive to pairing correlations and the high-j intruder orbitals.

To date, in-beam spectroscopic methods have been applied to study the isotopes of fermium and nobelium [2] with a recent study made on ^{256}Rf [3]. In the neutron-deficient even-even $N = 146$ isotones the ground-state rotational band has been measured in ^{238}U [4], ^{240}Pu [5], ^{242}Cm [6] and recently in ^{246}Fm [7] up to spin $I^\pi = 16^+$. However, information on the ground-state rotational band structure in the neutron-deficient californium isotopes only exist in the even-even ^{248,250,252}Cf [8] isotopes up to spins of 10^+, 12^+ and 10^+, respectively. Therefore, the structure of the ground-state rotational bands in californium are poorly known compared to the neighbouring elements in this region.

In this work we report on the first measurement of the ground-state rotational band in the even-even neutron-deficient isotope ^{244}Cf. This study contributes to the information on the heavy even-even $N = 146$ isotones and allows a systematic comparison of their behaviour and rotational properties.

* Corresponding author: joonas.konki@jyu.fi
† Present address: Physics Division, Argonne National Laboratory, Argonne, IL 60439, USA
‡ Present address: University of Liverpool, Department of Physics, Oliver Lodge Laboratory, Liverpool L69 7ZE, UK

II. EXPERIMENTAL SETUP AND METHODS

The neutron-deficient isotopes ^{244,243}Cf were produced as evaporation residues (ER) of the ^{246}Cf* compound nucleus formed in the fusion reaction ^{48}Ca+^{198}Pt. The experiment was carried out at the Accelerator Laboratory of the Department of Physics, University of Jyväskylä, Finland. The ^{48}Ca^{10+} ion beam was produced in an ECR ion source and accelerated in the K=130 MeV cyclotron before impinging on the enriched self-supporting ^{198}Pt targets of about 0.64 mg/cm^2 and 0.86 mg/cm^2 in thickness. The total time of the irradiation was about 220 h with typical beam intensities ranging from 20 to 40 pnA.

The ERs recoiling out of the target were separated from primary beam and target-like products by the gas-filled recoil separator RITU [9, 10] according to their magnetic rigidities. A carbon foil of thickness 0.04 mg/cm^2 was used as a charge-reset foil on the downstream side of the target to allow for a better separation of the primary beam from the ERs. The pressure of the helium gas inside the recoil separator was about 0.6 mbar.

Prompt γ rays that were produced at the target position were detected with the JUROGAMII array of 24 Clover-type [11] and 15 of either Phase-I [12] or GASP [13] type Compton-suppressed germanium detectors. The add-back method was used to determine the γ-ray energies deposited in the Clover detectors. In the current analysis two coincident events in diagonally opposite crystals in one detector were rejected. All other combinations of coincident events were summed.

The separated reaction products entering the focal plane detection chamber passed through a multi-wire proportional counter (MWPC) providing an energy-loss measurement (ΔE) and were implanted into two adjacent Double-sided Silicon Strip Detectors (DSSDs) of the GREAT focal-plane spectrometer [14]. In addition, the Time-of-Flight (ToF) between the MWPC and DSSDs was recorded. Each of the DSSDs was divided into 60 strips in the horizontal (X) direction and 40 strips in the vertical (Y) direction with a 1 mm strip pitch giving $120 \times 40 = 4800$ pixels in total. The thicknesses of the DSSDs were 300 µm. The DSSD channels were instrumented with analogue electronics. The vertical Y strips of the DSSDs were used with low gain to measure recoils and α particles, and the X strips were used with higher gain in order to measure low-energy internal conversion electrons. The DSSDs were surrounded by 28 silicon PIN diodes in a box configuration on the upstream side.

The Y strips of the DSSDs and the PIN detectors were calibrated with an external mixed three-line α source containing ^{239}Pu, ^{241}Am and ^{244}Cm and the X strips were calibrated using an external ^{133}Ba electron source. In order to match to the known energies of the most intense α decays from ^{240,242}Cm, 70 keV was subtracted from the measured α-particle energies to correct for the partially deposited recoil energy of the daughter nucleus in the α decay that is affected by the pulse-height defect. ^{240}Cm is produced in the α decay of ^{244}Cf. The energy resolution (full width at half maximum) of the DSSDs determined from the sum spectrum of all of the Y strips was approximately 25–30 keV at 7.05 MeV.

Two EUROGAM Clover-type [11] and one large-volume Clover-type germanium detectors were used to detect γ rays at the focal plane. A 15-mm thick double-sided Planar germanium strip detector with a 120×60 mm active area and a strip pitch of 5 mm was placed directly behind the DSSDs inside the same vacuum chamber. The Planar detector was used to detect X-rays and low-energy γ rays and as a veto detector to reject high-energy light particles that punch through the DSSDs. The germanium detectors were calibrated with ^{152}Eu and ^{133}Ba sources.

The energies of all events from the detectors were timestamped with a 100-MHz clock and recorded independently using the triggerless Total Data Readout (TDR) data-acquisition system [15]. All of the germanium and PIN detectors were instrumented with digital Lyrtech VHS-ADC cards. The γ-ray energies were determined using a Moving Window Deconvolution (MWD) algorithm [16] programmed in the field-programmable gate array (FPGA) circuit of the 14-bit ADC cards. The temporal and spatial correlations in the time-ordered data between the detectors were analysed using the GRAIN software package [17].

III. EXPERIMENTAL RESULTS

The ERs were selected on the basis of the measured ToF-E and ToF-ΔE matrices, where E is the energy deposited in the DSSDs and ΔE is the energy loss in the MWPC. The measured α-particle energy spectrum vetoed with the gas counter (MWPC) and the Planar detector is shown in Fig. 1 (a). The contaminant peak appearing at an energy of around 6.11 MeV was attributed to ^{242}Cm (E_α = 6.110(3) MeV [18]) originating from the α-decay chain starting from ^{254}No that was produced in a preceding experiment, and was present in the detector prior to this experiment. The other peaks in the measured spectra were assigned to ^{244}Cf (E_α = 7.21(2) MeV, $T_{1/2}$ = 19.4(6) min reported in [19] and E_α = 7.207(2) MeV, $T_{1/2}$ = 20.4(16) min in [20]), ^{243}Cf (E_α = 7.05(2) MeV, $T_{1/2}$ = 10.3(5) min reported in [19] and E_α = 7.06(1), 7.17(1) MeV, $T_{1/2}$ = 12.5(10) min in [20]) and ^{240}Cm (E_α = 6.290(5) MeV, $T_{1/2}$ = 27(1) d [21]) based on their α-particle energies and the observed half-lives (see Section III A). The aforementioned α-particle energies and half-lives are from the literature. In the present work the α-particle energies are only used in the recoil-decay tagging procedure and no attempt was made to improve the accepted values. For this reason the approximate calibration method described earlier was used.

It should be noted that in the work of Fields *et al.* [20] 7.06-MeV and 7.17-MeV α-particle energies were assigned to ^{243}Cf. Whereas, in Sikkeland *et al.* [19] only 7.05-MeV α-particle energy was observed and assigned

to ^{243}Cf but there is speculation that an α-particle group with an energy of 7.17 MeV could represent the α decay of ^{244}Cf to the excited 2^+ state in ^{240}Cm. In the present work the α peak assigned to ^{244}Cf has a low energy shoulder and thus could contain an additional 7.17-MeV component.

A search for a fusion-evaporation recoil implantation followed by an α decay in the same pixel of the DSSDs was made with a maximum search time of 100 min. The resulting recoil correlated α-particle energy spectrum is shown in Fig. 1 (b). The total numbers of correlated full-energy ER-α(^{244}Cf) and ER-α(^{243}Cf) pairs were about 2000 and 400, respectively.

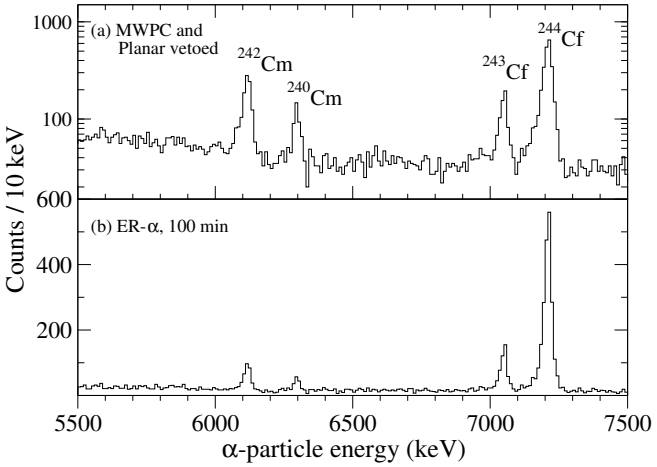

FIG. 1. Energy spectra of α particles from the ^{48}Ca + ^{198}Pt reaction measured in the DSSDs and vetoed with the gas counter (MWPC) and the Planar detector : (a) all α-like events; (b) α-like events following a recoil implantation at the same position in the DSSDs within 100 min.

Prompt γ ray singles measured at the target position with JUROGAMII and associated with the recoils that were correlated with the α decays of ^{244}Cf are shown in Fig. 2. The recoil-decay tagging (RDT) method [22, 23] had to be used instead of recoil-gating in order to obtain a clean prompt γ-ray energy spectrum corresponding to the produced ^{244}Cf nuclei. In addition, the PIN array of silicon detectors was used in the tagging procedure to improve the statistics in the γ-ray spectrum by detecting those α particles that escape the DSSDs depositing only part of their full energy which are then stopped in the PINs. The spectrum shows a sequence of transitions labeled with their transition energies with regular spacing that is characteristic of a rotational band of a deformed nucleus. The inset shows the γ rays up to an energy of 1 MeV with at least one peak at 704(1) keV that possibly originates from a side band feeding the low-spin states of the ground-state rotational band.

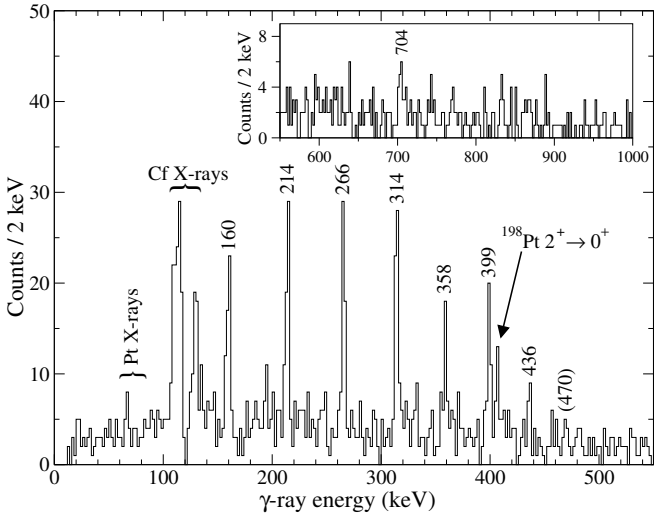

FIG. 2. Energy spectrum of prompt γ rays measured with the JUROGAMII array at the target position associated with the recoils tagged with ^{244}Cf α decays in the DSSDs and the escaped α particles observed in the PIN detectors. The inset shows the γ rays with energies up to 1 MeV.

A. Lifetimes and α-decay branching ratios

The measured ER-α time differences are shown up to $12 \cdot 10^3$ s in Fig. 3. In the cases of ^{244}Cf (Fig. 3(a)) and ^{243}Cf (Fig. 3(b)), α-particle energy gates of E_α = 7.12-7.27 MeV and E_α = 6.98-7.09 MeV have been applied, respectively. Double exponential functions were used to fit the measured ER-α time spectra of the form [24, 25]

$$f(t) = ae^{-(\lambda+r)t} + be^{-rt}, \quad (1)$$

where λ is the decay constant of the activity and r is the apparent decay constant of the component that arises from random correlations. These random correlations arise due to the manner in which the search is performed and the finite probability that an unwanted event can occur between the real recoil and α-particle event pair depending on the count rate of the individual pixels in the DSSDs. The half-lives obtained from the fits were $T_{1/2}$ = 19.3(12) min and $T_{1/2}$ = 10.9(5) min for ^{244}Cf and ^{243}Cf, respectively. The measured values are consistent within error bars with previously reported values [19] of $T_{1/2}$ = 19.4(6) min for ^{244}Cf and $T_{1/2}$ = 10.3(5) min for ^{243}Cf.

A measurement of the electron-capture (EC) decay branch in ^{244,243}Cf was not possible in this work due to the long half-lives and very low α-decay branching ratios of ^{244}Bk [26] ($T_{1/2}$ = 4.35(15) h, $b_\alpha = 6(2) \cdot 10^{-3}$%) and ^{243}Bk [27] ($T_{1/2}$ = 4.6(2) h, b_α = 0.1%). Therefore, an α-decay branching ratio of b_α = 14.0 % for ^{243}Cf that has been estimated in the literature [28, 29] using data from [19] and [20] was adopted. It should be noted that an estimate of EC/α = 10 is given in [19] because the assignment of the 7.17-MeV α particles to the α decay of

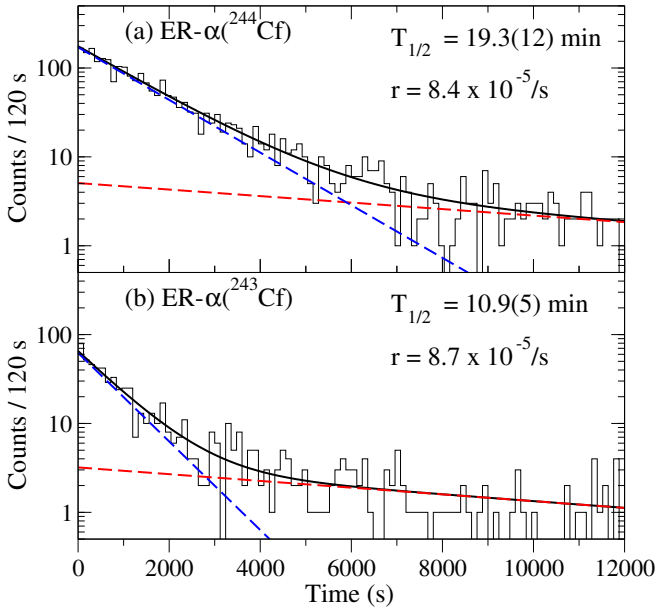

FIG. 3. (Color online) The measured ER-α times corresponding to (a) ^{244}Cf and (b) ^{243}Cf with a search time of up to $12{\cdot}10^3$ s. The dashed lines in blue (real) and red (random) correspond to the two components of the fitted decay curve that is shown in black (see text for more details).

^{243}Cf is questionable according to systematics [29].

The α-decay branching ratio of ^{244}Cf was estimated from experimental data from an earlier study of the decay properties of ^{248}Fm [30]. A value of $b_\alpha = 75(6)\,\%$ was determined by comparing the number of α decays from ^{248}Fm and ^{244}Cf from a gas-vetoed α-particle energy spectrum measured during the experiment that is shown in Fig. 4. The given uncertainty is only based on the determination of the peak areas. The systematic error caused by possible losses when the data acquisition was not collecting data of α decays from ^{244}Cf due to its long half-life was not taken into account. Therefore, the actual α-decay branch can be somewhat higher than the value given here.

B. Excitation functions

The production of ERs was measured as a function of the excitation energy of the compound nucleus ^{246}Cf* ranging from $E^* = 23$ up to 31 MeV. The beam was accelerated to energies of 207, 208, 211 and 213 MeV and two carbon foils with thicknesses of about 0.22 and 0.41 mg/cm^2 were used in front of the target for the reduction of beam energies in the 211-MeV runs. The thinner 0.64 mg/cm^2 target was used in the excitation function measurements. The excitation energies E^* were calculated by using the atomic mass data from AME2003 [31] and the LISE++ code [32], and correspond to the excitation energy at the centre of the target. The energy loss of the projectiles in the first half of the target was

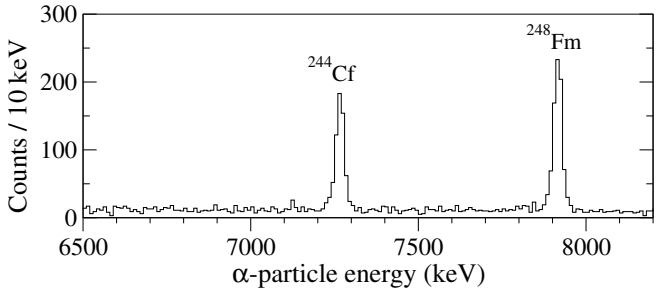

FIG. 4. Energy spectrum of α particles from the ^{48}Ca+^{202}Hg reaction measured in the DSSDs and vetoed with the gas counter (MWPC) from an earlier study of ^{248}Fm [30] that was used to determine the α decay branching ratio of ^{244}Cf. Note that the energies plotted on the x-axis have not been corrected for the partially detected recoil energy of the daughter nucleus (≈ 70 keV due to the pulse-height defect).

$\Delta E \approx 2.5$ MeV. The beam energies at the centre of the target correspond to excitation energies of the compound nucleus ^{246}Cf* of about 23(1), 26(1), 27(1), 30(1) and 31(1) MeV. In order to estimate the cross sections, the following factors were used: RITU transmission, DSSD coverage and DSSD full-energy α detection efficiency of 33(5) %, 83(5) % and 55(5) %, respectively. The beam dose was determined for each data point from an integral over the total rate of recoils observed at the focal plane. The rate was normalised to beam current values taken at times during the measurements using a Faraday cup and was used to monitor the possible target degradation during the irradiation. The main uncertainty in the data points comes from the beam dose estimate (20% uncertainty) and the uncertainty in RITU transmission. Only the uncertainty in the beam energy from the cyclotron (±0.5%) was taken into account in calculating the uncertainties in the excitation energies E^*. The α-decay branches of $b_\alpha = 75(6)\,\%$ and $b_\alpha = 14.0\,\%$ were used for ^{244}Cf and ^{243}Cf, respectively (see Section III A). The measured cross sections for the 2n and 3n evaporation channels are shown in Fig. 5. The maximum production cross sections of $\sigma(2n,\ max) = 120(40)$ nb and $\sigma(3n,\ max) = 170(80)$ nb were determined at excitation energies of about 26(1) MeV and 30(1) MeV, respectively.

C. Ground-state rotational properties of ^{244}Cf and moments of inertia

The measured transition energies of the ground-state rotational band in ^{244}Cf are shown in Table I with the tentative spin assignments and relative intensities corrected with the γ-ray detection efficiencies and internal conversion coefficients calculated using BrIcc [33] under the assumption that the transitions have an E2 character. Transitions up to the tentative spin and parity of $I^\pi = 20^+$ were identified. The rotational sequence up to

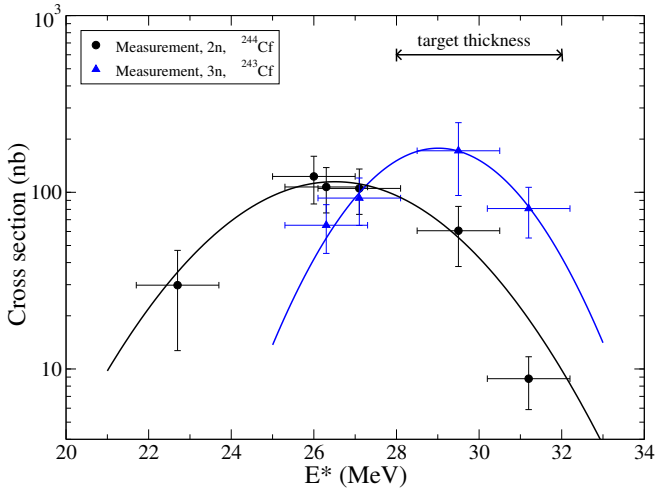

FIG. 5. (Color online) The measured cross sections for the 2n and 3n evaporation channels in the ^{48}Ca+^{198}Pt fusion reaction as a function of the excitation energy E^* at the centre of the target of the compound nucleus ^{246}Cf*. The solid lines are fits to guide the eye. See text for details.

$I^\pi = 18^+$ remains visible and the background is greatly reduced in γ-γ coincidence data and by gating on the transitions in the γ-γ matrix they are shown to be a cascade of coincident transitions. However, the γ-γ coincidence data can not be used to support the assignment of the 470-keV γ ray to the band, thus the assignment should be taken as tentative and based only on the intensity observed in the singles γ-ray spectrum. The 314-keV γ-ray transition is possibly a doublet because of the increased width and intensity of the transition. Therefore, two Gaussian functions with peak widths fixed to 2 keV were used to estimate the energy and area of the peak.

TABLE I. The measured transition energies and tentative assignments for the ground-state rotational band of ^{244}Cf. The extrapolated $4^+ \rightarrow 2^+$ and $2^+ \rightarrow 0^+$ transitions are also shown. The relative intensities have been corrected for γ-ray detection efficiency and internal conversion.

$J_i \rightarrow J_f$	E_γ (keV)	Relative intensity (%)
$(2^+ \rightarrow 0^+)$	45(1)[a]	
$(4^+ \rightarrow 2^+)$	103(1)[a]	
$(6^+ \rightarrow 4^+)$	160(1)	100(22)
$(8^+ \rightarrow 6^+)$	214(1)	60(10)
$(10+ \rightarrow 8^+)$	266(1)	54(8)
$(12^+ \rightarrow 10^+)$	314(1)[b]	30(10)
$(14^+ \rightarrow 12^+)$	358(1)	31(8)
$(16^+ \rightarrow 14^+)$	399(1)	33(11)
$(18^+ \rightarrow 16^+)$	436(1)	13(6)
$(20^+ \rightarrow 18^+)$	470(1)	7(6)

[a] Transition energy extrapolated from the Harris fit.
[b] Transition has been assumed to be a doublet.

The presence of the 407-keV γ ray originating from the Coulomb excitation of the target ($2^+_1 \rightarrow 0^+_{g.s.}$ transition in ^{198}Pt) makes estimating the peak area of the 399-keV transition challenging. The peak at 407 keV is very broad mostly due to the Doppler correction that is applied to the measured γ-ray energies in the JUROGAMII rings positioned at different angles with respect to the beam direction but also due to the straggling effects in the target and the fact that Coulomb excitation is a binary reaction. It should be noted that the 407-keV peak does not appear in the γ-γ coincidence data.

The $4^+ \rightarrow 2^+$ and $2^+ \rightarrow 0^+$ transitions in the ground-state rotational band could not be observed because they proceed mainly via internal conversion. In order to extrapolate the unobserved transition energies, the same procedure was used as in *e.g.* [3, 34] of parameterising the kinematic ($\mathcal{J}^{(1)}$) and dynamic ($\mathcal{J}^{(2)}$) moments of inertia of the rotational band according to the Harris formalism [35], where

$$\mathcal{J}^{(1)} = J_0 + J_1\omega^2, \tag{2}$$

$$\mathcal{J}^{(2)} = J_0 + 3J_1\omega^2. \tag{3}$$

The first observed transition of 160(1) keV was assumed in the fitting procedure to originate from a state with initial spin and parity of $I^\pi = 6^+$ that is typically observed in this region in the isotones as well as in the heavier region of the nuclear chart of nobelium and fermium, for example. Any other choice for the initial spin assignment of this transition would not give reasonable results from the fitting. The so-called Harris parameters (J_0, J_1) obtained from the fit to the low-spin part of the rotational band of ^{244}Cf using Eq. 2 were $J_0 = 67.3(2)\,\hbar^2\text{MeV}^{-1}$ and $J_1 = 250(10)\,\hbar^2\text{MeV}^{-3}$. The energies of the $4^+ \rightarrow 2^+$ and $2^+ \rightarrow 0^+$ transitions were estimated using these parameters and the formula

$$I = J_0\omega + J_1\omega^3 + 1/2, \tag{4}$$

where I is the initial angular momentum of the transition. The transition energies obtained for the two lowest transitions in the rotational band were $E_\gamma(4^+ \rightarrow 2^+) = 103(1)$ keV and $E_\gamma(2^+ \rightarrow 0^+) = 45(1)$ keV.

It should be noted that the 103-keV region in the α-tagged γ-ray spectrum of Fig. 2 is clean from background and does not show a peak from a possible 103-keV $(4^+ \rightarrow 2^+)$ transition. In addition, the intensity ratio of the Cf K_α/K_β X-rays does not show an excess of counts from a possible contribution of a 103-keV γ-ray transition that could overlap with the K_α peaks. On the other hand, the internal conversion coefficient calculated with BrIcc [33] for the transition assuming an E2 character is 19.4(10) which implies that only few γ rays could be observed with the level of statistics that is available in this work. Therefore, the assignment of a 103-keV transition to $4^+ \rightarrow 2^+$ is not inconsistent because the transition is highly converted.

IV. DISCUSSION

The first observation of the ground-state rotational band in ^{244}Cf and the estimate of the excitation energy of the first 2^+ state shows that it has a similar deformation to other nuclei in the region. In fact, prolate quadrupole deformation parameters (β_2) of 0.24 [36] and 0.25 [37] have been calculated for the ground state of ^{244}Cf. The measurement of the transitions in the band up to $I^\pi = 20^+$ allows a comparison to be made with other heavy even-even neutron-deficient $N = 146$ isotones and their rotational properties.

A. Systematics of the N=146 isotones

The kinematic $\mathcal{J}^{(1)}$ and dynamic $\mathcal{J}^{(2)}$ moments of inertia of the ground-state rotational bands as a function of the rotational frequency ($\hbar\omega$) in the even-even N=146 isotones are shown in Fig. 6(a) and 6(b), respectively. The results from this work on ^{244}Cf are compared to that of ^{238}U [4], ^{240}Pu [5], ^{242}Cm [6] and ^{246}Fm [7]. The lines are drawn using Eq. 2 and 3 and the Harris parameters that were obtained from fits made to the low-spin part of the measured $\mathcal{J}^{(1)}$ data of each nucleus.

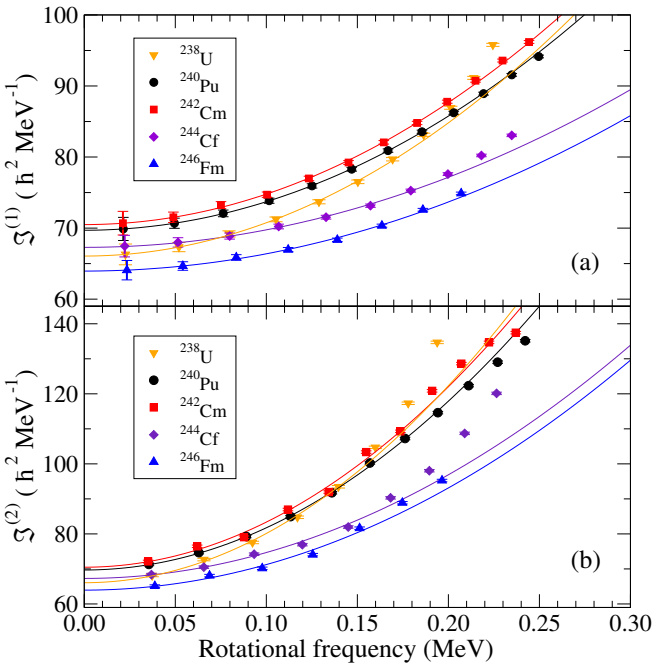

FIG. 6. (Color online) The (a) kinematic $\mathcal{J}^{(1)}$ and (b) dynamic $\mathcal{J}^{(2)}$ moments of inertia of the ground-state rotational bands as a function of rotational frequency ($\hbar\omega$) in the even-even N=146 isotones ^{238}U [4], ^{240}Pu [5], ^{242}Cm [6], ^{244}Cf (from this work) and ^{246}Fm [7]. The lines represent (a) fits to the low-spin part of the $\mathcal{J}^{(1)}$ data using the γ-ray transition energies with Eq. 2 and (b) $\mathcal{J}^{(2)}$ plotted using Eq. 3 and the Harris parameters obtained in (a). See text for details.

The absolute values of the kinematic moments of inertia at low spin are closely related to the energy of the first excited 2^+ state. In turn, the energy of the 2^+ state can be related to the quadrupole deformation or in the region of the deformed shell gaps to the pairing correlations, which are reduced [36]. The reduction in the pairing correlations result in an increase in the moment of inertia. Fig. 6(a) shows the kinematic moments of inertia of the $N = 146$ isotones where ^{242}Cm has the highest value at low spin just above that of ^{240}Pu. The $\mathcal{J}^{(1)}$ value of ^{244}Cf obtained in this work is closer to and only a little higher than that of ^{238}U. Finally, ^{246}Fm has the lowest $\mathcal{J}^{(1)}$ value of the group. More interesting features are revealed by comparing the behaviour of the dynamic moment of inertia in these isotones.

From the $\mathcal{J}^{(2)}$ data shown in Fig. 6(b) it is evident that there is a sharp increase in the dynamic moment of inertia in ^{244}Cf at a rotational frequency of about $\hbar\omega = 0.20$ MeV. A similar up-bend has been observed clearly in ^{238}U and is very likely to occur also in ^{246}Fm based on the highest transitions that have been observed in the ground-state band and the next tentative transition in the band [38]. In contrast, ^{242}Cm and ^{240}Pu that have a higher kinematic moment of inertia $\mathcal{J}^{(1)}$ do not show any signs of up-bend in the dynamic moment of inertia $\mathcal{J}^{(2)}$ up to rotational frequencies as high as $\hbar\omega = 0.25$ MeV. One possible physical explanation for the up-bending behaviour is the alignment of coupled protons or neutrons in the high-j orbitals to the rotational axis of the nucleus due to the Coriolis effect.

It has been shown experimentally by g-factor measurements that the up-bend at $\hbar\omega \approx 0.25$ MeV of the ground-state band in ^{238}U results from the alignment of a pair of protons in the $i_{13/2}$ orbital according to [39, 40]. Additionally, in [41] it has been shown that in the $N = 151$ isotones of ^{245}Pu, ^{247}Cm and ^{249}Cf the alignment behaviour is mostly caused by $i_{13/2}$ protons on the basis of neutron orbital blocking arguments. Similar results were proposed in [6] on ^{241}Cm ($N = 145$) and ^{237}Np ($N = 144$) based on blocking arguments. In [42] the alignment in ^{235}Np ($N = 142$) was studied and the role of $j_{15/2}$ neutrons has been proposed, although, the proton contribution could not be ruled out. Therefore, it seems that in most cases the alignment effects are in fact caused by the protons active in high-j orbitals and experimental evidence for the neutrons contributing to the alignment effect is sparse or not conclusive. In theoretical calculations on the rotational properties such a clear distinction between the proton and neutron alignment is not evident, as discussed further in the next section.

B. Theoretical estimates

Only a few recent calculations have been made on the rotational properties of the ground-state bands in the region of the heavy $N = 146$ isotones.

In Afanasjev *et al.* [43] the cranked relativistic Hartree-Bogoliubov theory has been applied to perform exten-

sive calculations in the actinides and light superheavy elements including the heavy $N = 146$ isotones. The absolute values of $\mathcal{J}^{(1)}$ and the relative differences between all of the $N = 146$ isotones are rather well reproduced at low spin. However, an up-bend is predicted in all of the isotones by the calculations and the up-bend in ^{238}U and ^{240}Pu is predicted to occur at lower rotational frequency than in ^{242}Cm, ^{244}Cf and ^{246}Fm. Furthermore, in all of the cases the calculations indicate that both the neutron and proton contributions to the alignment occur simultaneously at the same frequency. The $\mathcal{J}^{(1)}$ of ^{244}Cf as a function of the rotational frequency calculated using the NL3* parametrisation is shown in Fig. 7 with the contributions from the neutrons (blue) and protons (red) shown in the inset.

It has been suggested that the non-observation of the alignment in ^{240}Pu is due to strong octupole correlations [44] that have not been taken into account in the calculations. Likewise, a self-consistent mean field calculation of ^{240}Pu with the SLy4 interaction does not include octupole correlations and predicts an up-bend in $\mathcal{J}^{(2)}$ [45]. It is interesting to note that in [46] a non-zero octupole deformation (β_3) is predicted for the ground state of ^{242}Cm and ^{240}Pu as well as for ^{238}U by using the relativistic Hartree-Bogoliubov and covariant density functional theory. Despite the possibly similar calculated octupole deformations in their ground states, experimentally ^{238}U shows alignment effects at high rotational frequencies, whereas, ^{240}Pu and ^{242}Cm do not.

Another theoretical study on the even-even actinides has been made by Delaroche *et al.* [47] using the cranked Hartree-Fock-Bogoliubov method with the Gogny D1S force. In their work, the experimentally observed up-bend in ^{244}Cf is not predicted. In the case of ^{240}Pu an up-bend is again predicted possibly due to the missing treatment of the octupole correlations. In ^{246}Fm the predicted up-bend is delayed up to a rotational frequency of $\hbar\omega \approx 0.30$ MeV. The calculated results are consistent with experimental results for ^{238}U showing an up-bend at $\hbar\omega \approx 0.20$ MeV and no alignment features in ^{242}Cm at $\hbar\omega \leq 0.30$ MeV.

In a recent theoretical study of nuclei in the ^{252,254}No region [48] the up-bend in ^{246}Fm at $\hbar\omega \approx 0.20$ MeV is predicted correctly, although, the absolute value of $\mathcal{J}^{(1)}$ at low-spin is overestimated. In that work, Total Routhian Surface calculations based on the cranked shell model including pairing correlations were made. Another calculation with spectroscopic quality energy-density functionals based on the Skyrme Hartree-Fock-Bogoliubov and Lipkin-Nogami methods has been made to calculate the rotational bands of nuclei in the nobelium region [49]. Their calculations included ^{246}Fm and an up-bend was predicted in its ground-state band. Unfortunately, the calculations reported in the latter two studies did not include the lighter $N = 146$ isotones that are discussed in this work.

Following the same theoretical methods and framework as used in [49], calculations were performed for the ground-state band of ^{244}Cf. The results for the kinematic $\mathcal{J}^{(1)}$ moment of inertia from the calculation are shown with a dashed black line in Fig. 7 together with the measured data points from this work. Calculated data from [43] is included in the same figure with a dash-dotted red line. It is evident, that the up-bend in $\mathcal{J}^{(1)}$ is predicted by both calculations. According to [43], the alignment would occur at the same frequency for protons and neutrons and that the neutrons have a larger contribution. Strikingly, the absolute value of $\mathcal{J}^{(1)}$ at low spin is very close to the experimental value and well within the uncertainties. The quadrupole deformation parameter extracted from the calculations was $\beta_2 = 0.26$.

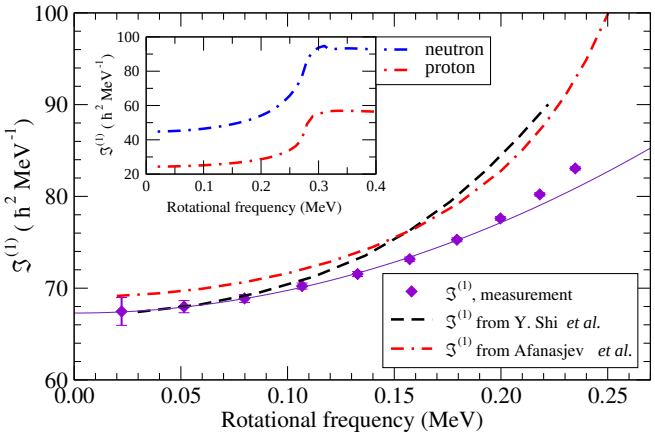

FIG. 7. (Color online) The kinematic $\mathcal{J}^{(1)}$ moment of inertia of the ground-state rotational band in ^{244}Cf as a function of the rotational frequency ($\hbar\omega$). The measured values from this work are compared to calculations from Afanasjev *et al.* [43] using the NL3* parametrisation (dash-dotted red line) with the inset showing the calculated neutron (blue) and proton (red) contributions. Calculations performed in a similar way as described in Y. Shi *et al.* [49] (dashed black line) are also included. The solid line represents a fit to the low-spin part of the $\mathcal{J}^{(1)}$ data using the measured γ-ray transition energies with Eq. 2. See text for details.

In all of the available extensive calculations [43, 45, 47] both neutrons and protons in high-j orbitals align simultaneously at the same rotational frequency and contribute to the up-bend in the the dynamic moment of inertia. On the contrary, measurements to date have shown no clear evidence for neutron alignments and that only protons in high-j orbitals are responsible for the alignment.

V. SUMMARY

In summary, the neutron-deficient californium nuclei ^{244}Cf and ^{243}Cf were produced in the fusion-evaporation reactions ^{198}Pt(^{48}Ca,2n)^{244}Cf and ^{198}Pt(^{48}Ca,3n)^{243}Cf, respectively. The excitation functions of the two reaction channels were measured. The half-lives of ^{244}Cf and ^{243}Cf were determined from the ER-α correlations to be $T_{1/2} =$

19.3(12) min and $T_{1/2} = 10.9(5)$ min, respectively. The α-decay branch of ^{244}Cf was assessed to be $b_\alpha = 75(6)\,\%$ by using data from a previous experiment. The excited states in the $Z = 98$ nucleus ^{244}Cf were studied for the first time and the ground-state rotational band up to tentative $I^\pi = 20^+$ was identified using in-beam γ-ray spectroscopy. The deduced moments of inertia of the band indicate an up-bend due to a possible alignment of nucleons in high-j orbitals at a frequency of about $\hbar\omega = 0.20$ MeV. The results were compared to other even-even $N = 146$ isotones as well as to theoretical calculations where available.

The statistics obtained in this work for ^{243}Cf were not sufficient to associate prompt γ-ray transitions to this nucleus. This was due to the low α-decay branch that did not allow to take full advantage of the use of the recoil-decay tagging method. It would be interesting to try to disentangle the complex level-scheme structure of this odd-A nucleus and to study its poorly known decay properties with higher statistics in a future experiment.

More calculations including the effects of octupole correlations are needed in this region in order to understand and reproduce the experimentally observed alignment properties in the $N = 146$ isotones.

ACKNOWLEDGMENTS

J. Konki acknowledges support from the Alfred Kordelin Foundation. The use of the GAMMAPOOL loan pool germanium detectors is acknowledged. This work has been supported by the Academy of Finland under the Finnish Centre of Excellence Programme (2012-2017) and by the Academy of Finland and University of Jyväskylä within the FIDIPRO program. Support has also been provided by the EU 7th Framework Programme Project No. 262010 (ENSAR) and by the Espace de Structure Nucléaire Théorique (CEA/DSM-DAM). Authors wish to thank A. V. Afanasjev for providing additional information and data from their work.

[1] R.-D. Herzberg and P. T. Greenlees, Prog. Part. Nucl. Phys. **61**, 674 (2008).
[2] Ch. Theisen *et al.*, Nucl. Phys. A **944**, 333 (2015).
[3] P. T. Greenlees *et al.*, Phys. Rev. Lett. **109**, 012501 (2012).
[4] D. Ward *et al.*, Nucl. Phys. A **600**, 88 (1996).
[5] G. Hackman *et al.*, Phys. Rev. C **57**, R1056 (1998).
[6] K. Abu Saleem *et al.*, Phys. Rev. C **70**, 024310 (2004).
[7] J. Piot *et al.*, Phys. Rev. C **85**, 041301(R) (2012).
[8] R. Takahashi *et al.*, Phys. Rev. C **81**, 057303 (2010).
[9] M. Leino *et al.*, Nucl. Inst. Meth. Phys. Res. B **99**, 653 (1995).
[10] J. Sarén *et al.*, Nucl. Inst. Meth. Phys. Res. A **654**, 508 (2011).
[11] G. Duchêne *et al.*, Nucl. Inst. Meth. Phys. Res. A **432**, 90 (1999).
[12] C. W. Beausang *et al.*, Nucl. Inst. Meth. Phys. Res. A **313**, 37 (1992).
[13] C. Rossi Alvarez, Nuclear Physics News **3**, 10 (1993).
[14] R. D. Page *et al.*, Nucl. Inst. Meth. Phys. Res. B **204**, 634 (2003).
[15] I. H. Lazarus *et al.*, IEEE Trans. Nucl. Sci **48**, 567 (2001).
[16] A. Georgiev and W. Gast, IEEE Trans. Nucl. Sci **40**, 770 (1993).
[17] P. Rahkila, Nucl. Inst. Meth. Phys. Res. A **595**, 637 (2008).
[18] F. Asaro *et al.*, Phys. Rev. **87**, 277 (1952).
[19] T. Sikkeland *et al.*, Phys. Lett. **24B**, 333 (1967).
[20] P. R. Fields *et al.*, Phys. Lett. **24B**, 340 (1967).
[21] B. Singh and E. Browne, Nuclear Data Sheets **109**, 2439 (2008).
[22] K.-H. Schmidt *et al.*, Phys. Lett. B **168**, 39 (1986).
[23] E. S. Paul *et al.*, Phys. Rev. C **51**, 78 (1995).
[24] M. Leino, S. Yashita, and A. Ghiorso, Phys. Rev. C **24**, 2370 (1981).
[25] A. Chatillon *et al.*, Eur. Phys. J. A **30**, 397 (2006).
[26] A. Chetham-Strode, Jr., Ph.D. thesis, University of California (1956), UCRL-3322.
[27] S. G. Thompson *et al.*, Phys. Rev **80**, 781 (1950).
[28] C. D. Nesaraja and E. A. McCutchan, Nuclear Data Sheets **121**, 695 (2014).
[29] E. Browne and J. K. Tuli, Nuclear Data Sheets **122**, 293 (2014).
[30] S. Ketelhut, Ph.D. thesis, University of Jyväskylä (2010).
[31] G. Audi *et al.*, Nucl. Phys. A **729**, 337 (2003), the 2003 NUBASE and Atomic Mass Evaluations.
[32] O. B. Tarasov *et al.*, Nucl. Phys. A **746**, 411c (2004), `http://lise.nscl.msu.edu/`.
[33] T. Kibédi *et al.*, Nucl. Inst. Meth. Phys. Res. A **589**, 202 (2008), `http://bricc.anu.edu.au/`.
[34] B. Sulignano *et al.*, Phys. Rev. C **86**, 044318 (2012).
[35] S. M. Harris, Phys. Rev. **138**, B509 (1965).
[36] A. Sobiczewski, I. Muntian, and Z. Patyk, Phys. Rev. C **63**, 034306 (2001).
[37] P. Möller *et al.*, Atomic Data and Nuclear Data Tables **109–110**, 1 (2016).
[38] J. Piot, (private communication).
[39] S. Zhu *et al.*, Phys. Rev. C **81**, 041306(R) (2010).
[40] O. Häusser *et al.*, Phys. Rev. Lett. **48**, 383 (1982).
[41] S. S. Hota *et al.*, Phys. Lett. B **739**, 13 (2014).
[42] A. M. Hurst *et al.*, Phys. Rev. C **81**, 014312 (2010).
[43] A. V. Afanasjev and O. Abdurazakov, Phys. Rev. C **88**, 014320 (2013).
[44] I. Wiedenhöver *et al.*, Phys. Rev. Lett. **83**, 2143 (1999).
[45] M. Bender *et al.*, Nucl. Phys. A **723**, 354 (2003).
[46] S. E. Agbemava, A. V. Afanasjev, and P. Ring, Phys. Rev. C **93**, 044304 (2016).
[47] J.-P. Delaroche *et al.*, Nucl. Phys. A **771**, 103 (2006).
[48] H. L. Liu, F. R. Xu, and P. M. Walker, Phys. Rev. C **86**, 011301 (2012).
[49] Y. Shi, J. Dobaczewski, and P. T. Greenlees, Phys. Rev. C **89**, 034309 (2014).